Detecting shape change: Characterizing the interaction between texture-defined and contour-defined borders

Ken W. S. Tan
The University of Western Australia, School of Psychology, Crawley, Western Australia, Australia

J. Edwin Dickinson
The University of Western Australia, School of Psychology, Crawley, Western Australia, Australia

David R. Badcock
The University of Western Australia, School of Psychology, Crawley, Western Australia, Australia

The human visual system's extreme sensitivity to subtle changes in shape can often be attributed to global pooling of local information. This has been shown for shapes described by paths of contiguous elements, but it was unknown whether this global pooling translated to shapes defined by texture-segmentation borders. Also, previous research suggests that texture and luminance cues-to-shape are integrated by the visual system for shape detection but it has not been established whether they combined for shape discrimination. Controlled shapes defined either by an explicit path of Gabors, texture-segmentation borders, or both of these cues were used. Results show that all stimuli used were globally processed. Thresholds for shapes defined by both cues matched predictions based on an independent-cue vector sum of individual thresholds. Thus, while local elements are integrated around the contour and are processed by global shape-detection mechanisms, integration did not occur across different shape-cues.

Introduction

Objects are commonly differentiated by many visual properties. Being able to efficiently exploit such diverse cues is likely to be advantageous to an individual, as this would allow them to utilize object information from more than one stimulus dimension in their identification (Hussain, Sekuler, & Bennett, 2011). Landy, Banks, and Knill (2011) note that sensory information varies along different dimensions but that if one of these cues provided a flawless estimate of an object property, then the need for any other cues would be irrelevant. Unfortunately, visual cues are rarely perfectly informative, with each cue providing different information and the neural signal being further degraded by noise intrinsic to the visual system. It is proposed that by combining multiple cues, the observer is generally able to obtain a more reliable estimate of an object property (Landy et al., 2011). The question addressed here is whether commonly available cues are actually combined when the visual system is judging differences in shape.

The boundaries of shapes can be defined by segmentation based on different cues, luminance, texture, motion, color, and binocular disparity have all been noted in a review by Regan (2000). A common form of boundary seen in the natural world is defined by a luminance change at the boundary, although such contours are often incomplete due to variation in lighting, shadow, or occlusion by other objects (Marr & Hildreth, 1980). Such a boundary will be described as luminance-defined. This can either be seen when a border of different luminance (i.e., a line) defines a shape, or when luminance changes at a boundary (i.e., an edge). Boundaries can also be specified in the absence of a change in local average luminance, such as when texture changes at a boundary (Barbot, Landy, & Carrasco, 2012).

Bergen (1991) suggests that the term "texture" can be generalized to indicate the characteristics of an object

Citation: Tan, K. W. S., Dickinson, J. E., & Badcock, D. R. (2013). Detecting shape change: Characterizing the interaction between texture-defined and contour-defined borders. *Journal of Vision, 13*(14):12, 1–16. http://www.journalofvision.org/content/13/14/12, doi: 10.1167/13.14.12.

doi: 10.1167/13.14.12 Received December 04, 2012; published December 16, 2013 ISSN 1534-7362

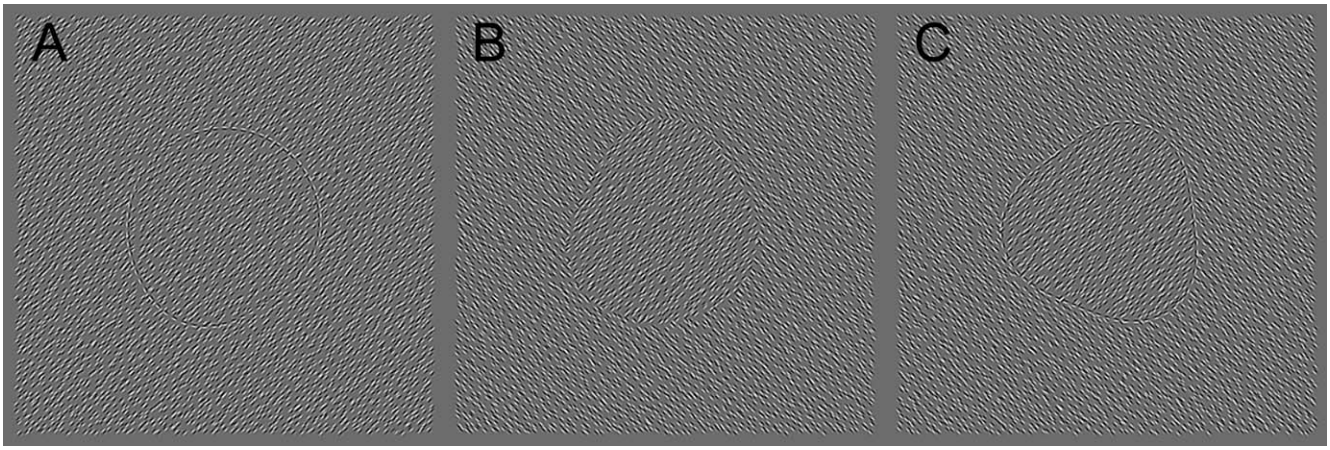

Figure 1. Examples of the three conditions used in Experiments 1 and 2, also illustrating different numbers of CoM (1–3, left to right). In Experiment 1, the number of CoM was varied (1, 2, and 3 CoM) for each condition, while in Experiment 2, 3 CoM always appeared. (A) GP shapes defined by a contiguous arrangement of Gabor patches (shown with 1 CoM), (B) TB shapes defined by texture-segmentation boundaries (shown with 2 CoM), and (C) PTB shapes defined by both an explicit Gabor path and texture-segmentation boundary (shown with 3 CoM). RF patterns shown here are at modulation amplitudes well above discrimination thresholds.

arising from the arrangement or attributes of its particles or constituent parts. Texture is a familiar cue since most objects are comprised of textures bounded by a luminance-defined edge (Ramachandran, Gregory, & Aiken, 1993). For texture to serve as a cue to shape, a difference in texture inside and outside of the boundary of the object is required. When an area of texture is surrounded by, and forms a boundary with, another area of differing texture (see Figure 1B), it can result in the shape of the embedded texture seeming as though it has "popped out" from the background. This is known as texture-segmentation and is an apparently effortless partition of a visual stimulus into distinct sections based on spatial gradients in local feature properties (Heinrich, Andrés, & Bach, 2007). The question of central interest here is whether global contour integration applies to such borders.

Since texture-segmentation occurs despite the lack of luminance edges, it is apparent that this segmentation can be based on the analysis and comparison of specific texture properties in parts of the pattern (Nothdurft, Gallant, & Van Essen, 2000). Of these properties, orientation, size, and contrast are examples that have been independently observed as being capable of allowing segmentation to occur (Julesz, 1981; Landy & Bergen, 1991; Malik & Perona, 1990; Nothdurft, 1993; Nothdurft et al., 2000; Thielscher & Neumann, 2003).

Orientation's role as a texture cue has received considerable attention over the years. Nothdurft (1985) found that when organized line segments were used as texture, performance in shape identification improved as differences in the orientation of the lines in the foreground and background increased. He also argued that texture-segmentation occurred not because of the grouping resulting from the homogeneity of feature elements but rather by the detection of boundaries defined by adequate contrast along a particular attribute dimension. This was further supported by a later single cell recording study (Nothdurft et al., 2000) that showed that when macaques were presented with textures with regions where texture-segmentation occurred, neurons tuned for orientation in V1 were more active near texture borders than within regions of homogenous texture. However, the studies by Nothdurft and his colleagues did not require the detection of subtle shape changes and did not attempt to determine whether contour information was globally integrated.

The ability to single out one of a group of items in a scene requires observers to be able to differentiate between the target item and its distractors. While there is usually a large array of potential discriminating cues, recognizing the shape of an object has been shown to be pivotal for determining an object's identity (Biederman, 1987). Using functional magnetic resonance imaging (fMRI), Kourtzi and Kanwisher (2000) observed an overlap of activation in high-order cortical areas when participants were asked to view pictures of grayscale objects and line drawings (of the same objects); while viewing pictures of scrambled counterparts of these objects did not activate the same areas. The line drawings lacked information from other feature dimensions that the grayscale images contained, yet overlapping cortical activation (of equal strength) was observed, implying a significant role for connected boundaries in shape specification within these cortical regions.

While it has been shown that synthetic images without texture rarely look realistic (Bergen, 1991), the activation in lateral occipital cortex (LOC) measured by Kourtzi and Kanwisher (2000) during a shape-

detection task was very similar for grayscale images and line drawings, suggesting a prominent contour is sufficient in their task. However, their task did not require subtle shape discrimination where multiple cues may be beneficial in combination.

Regan and Hamstra (1992) have shown that the human visual system is extremely sensitive to differences in the shape of borders, with the ability to discriminate between circles and ellipses with positional differences in contours of only seven arcseconds. The focus here is in determining how cues to texture and luminance differences are combined when judging subtle differences in shape to see if any additional benefit was derived from the addition of texture. Most previous research looking at stimuli with texture were investigating whether the stimuli segmented or not (Caputo, 1996; Harrison & Keeble, 2008; Heinrich et al., 2007) without making precise shape judgments. The current study examines how subtle changes to texture- and luminance-defined cues to shape affected the ability to make shape judgments when the shapes are defined by radial frequency patterns, and whether both support global integration of contour information.

Radial frequency (RF) patterns are a stimulus type that has been introduced to examine human visual processing of shape and one that supports a simple method for directly testing for global contour integration (Wilkinson, Wilson, & Habak, 1998). They are created by sinusoidally modulating the radius of a circle as a function of polar angle, where the RF number denotes the number of complete cycles of modulation of the radius necessary to complete 360° (for more detail see Wilkinson et al., 1998). Thresholds for detecting deformation (shape change) improve as more cycles of modulation (CoM) are added progressively to an otherwise circular contour. This could arise from the increased likelihood of detecting local cues when there are more of them (probability summation; Quick, 1974). However, the rate of improvement in thresholds as more CoM of a specified wavelength are added and observed for low frequency RF patterns is greater than that expected for probability summation. This rate of decrease in threshold has been used as a marker for integration or global pooling of deformation information around the pattern, and is found with low frequency RF patterns (less than 8–10 cycles of modulation in 360°) (Bell & Badcock, 2008; Hess & Field, 1999; Jeffrey, Wang, & Birch, 2002; Loffler, Wilson, & Wilkinson, 2003) where active integration of the local information around the contour shape is observed (Jeffrey et al., 2002). There are likely to be several steps in the processing of shape leading to the global integration stage. Initially, local orientation and position of contour elements must be detected (Field, Hayes, & Hess, 1993; Loffler, 2008). It is likely that these local elements are then combined into local curvature estimates (Badcock, Almeida, & Dickinson, 2013; Bell, Gheorghiu, Hess, & Kingdom, 2011; Loffler, 2008; Poirier & Wilson, 2006, 2010; Zwickel, Wachtler, & Eckhorn, 2007) before being processed as a global shape where the curvature maxima and polar angles separating them have been shown to be salient properties for the global integration process (Bell, Dickinson, & Badcock, 2008; Dickinson, Bell, & Badcock, 2013).

Global pooling has been demonstrated to occur when using stimuli defined by an explicit boundary specified by luminance difference (both as a continuous path and a sampled path) (Bell & Badcock, 2008; Dickinson, Han, Bell, & Badcock, 2010; Loffler et al., 2003). However, to the best of our knowledge, this phenomenon has not been shown to occur in shapes defined by texture-segmentation boundaries. In this study, we compared the discrimination thresholds for radial frequency (RF) patterns, which were chosen because there is an explicit marker for detecting global integration, specified by: (a) an explicit path of Gabor patches (luminance-defined sinusoidal gratings localized by a Gaussian contrast window) within a uniform background texture (Gabor path [GP]), (b) differences in texture with no explicit path (texture-segmentation boundary [TB]), and (c) a combination of both (Gabor path and texture-segmentation boundary [PTB]). Should shapes defined by texture differences be processed globally like GP defined shapes, it would be expected that thresholds for the TB stimulus should fall at a rate that exceeds probability summation as the number of CoM is increased.

It has been noted that a sensory system such as the visual system can benefit from including different features from the one sensory input (Landy et al., 2011). In line with the notion of using different features in a single sensory input, we looked at trying to understand whether shape discrimination was improved with the presence of texture. There are several ways in which a stimulus with both texture and explicit boundaries might be processed: (1) The cues are processed separately (locally and then globally) and the visual system treats each global signal as making an independent contribution; (2) the cues are detected by a common local mechanism combining information for both cues at each point, and then the local information is processed globally; and (3) the local cues are processed separately and then fed into a common global mechanism once they are processed. Options 2 and 3 result in a combined signal at the global level, while Option 1 results in independent signals at the global level. This study investigates how information is combined at the global level in order to help choose between these options. A combined input at the global

level incorporating the strength of the local cues would result in the threshold being inversely proportional to the strength of all cues present, while an independent input at the global level would be demonstrated by a probabilistic improvement in threshold due to the improved chance of detection of one of two cues present. Machilsen and Wagemans (2011) have conducted a recent study looking at the combination of surface and contour cues. A detection task with shapes created by combining several radial frequency components defined by either an explicit boundary, composed of appropriately aligned Gabor patches; a texture boundary, composed of a common orientation of Gabor elements in a random orientation surround; or a combination of both cues was employed. The observer's task was to detect the presence of a shape (the nontarget interval contained random orientation components). The authors manipulated the amount of orientation jitter in the elements to degrade the border and found that, as orientation jitter increased, the proportion of correct responses fell. They also observed that their double-cue stimuli had an accuracy advantage over both their single cue stimuli, which they found was consistent with the integration of both cues for the decision as to the presence of a shape. One concern with this task is that the detection of any level of coherent orientation cues, either aligned for the path or a region with similar orientations for the texture, would signal the target interval. This is potentially a common cue for both stimulus types and does not require precise shape discrimination. Thus, the combination of information observed might not directly reflect the properties of shape integration processes.

As with the previous study (Machilsen & Wagemans, 2011), we expected the PTB stimulus that had both a texture-segmentation boundary and an explicitly defined Gabor path to have threshold values that were lower than GP and TB individually. While the previous study found that these cues were integrated for the detection of the presence of a shape, we wished to know whether this integration of boundary cues also occurred for shape discrimination where subtle changes in border location are critical. If texture-segmentation boundaries and explicit paths of Gabor elements were processed separately, discrimination ability would only increase as a result of the increased probability of detecting a cue (from multiple cues). This decrease in threshold could be predicted by an orthogonal vector summation (Massof & Starr, 1980). However, if the two boundaries were pooled into the same discrimination mechanism, the system should benefit from having an increased amount of information in the same channel. This decrease in threshold should then exceed the probability summation prediction and could then be predicted by a linear summation of sensitivity. For purposes of the current study, the summing of unrelated cues in an orthogonal manner will be referred to as an independent prediction, and the summing of related cues in a linear manner will be referred to as the addition prediction.

To recapitulate, the first question in this study looked at replicating the results of previous literature suggesting global integration of local information around a shape for explicit contours defined by a contiguous path and comparing those to texture-segmentation boundaries to see whether shapes defined by texture-segmentation were also globally pooled. Global integration was to be demonstrated by having steeper threshold slopes relative to a probability summation prediction—one that explained increased performance due to the increased probability of detecting a single CoM as the total number of CoM increased around the shape. The second question examined whether these two types of contours were pooled into a single mechanism or whether they acted as independent cues to discrimination of shape. Probability summation in this instance explains the increased performance as arising from the increased probability of detecting one cue as the number of (global) cues present increased. The outcomes in this shape discrimination task differ from those obtained by Machilsen and Wagemans (2011) in their shape detection task, even though the stimuli have some similarities.

General methods

Participants

Five experienced psychophysical observers participated, two of which were authors; all other participants were naïve to the experimental aims. All participants reported normal or corrected-to-normal visual acuity. One of the participants has a divergent squint and, despite possessing normal visual acuity in both eyes, completed all testing monocularly by covering one eye with an opaque eyepatch; all other participants were tested binocularly. Participation was voluntary and informed consent was obtained prior to the commencement of testing. Two of the participants were reimbursed the costs of attending sessions ($10/session). All experiments complied with the guidelines set by the Human Research Ethics Committee of the University of Western Australia and were in accordance with the tenets of the Declaration of Helsinki.

Apparatus

Custom stimuli were generated using MATLAB 7.0.4 (MathWorks, Natick, MA, USA) on an Intel®

Pentium® 4 CPU 3.0 GHz (1024 MB RAM) and presented on a Sony Trinitron Multiscan G520 Monitor (screen resolution: 1024 × 768 [34°8′ × 25°36′], refresh rate: 100 Hz) from a 265 MB frame store of a Cambridge Research Systems ViSaGe graphics system. A chinrest was used to maintain a viewing distance of 65.5 cm. At this distance, each pixel subtended 2′ of visual angle. Testing occurred in a darkened room (ambient luminance $<1 cd/m^2$). Screen luminance was calibrated with an Optical OP 200-E photometer (Head model #265) and associated software (Cambridge Research Systems, Kent, UK). The space-averaged mean luminance and background to the stimuli was set at $45 cd/m^2$. A Cambridge Research Systems CB6 Response Box was used to record observer responses.

Stimuli

Three different conditions were run: Gabor path (GP), texture-segmentation boundary (TB), and one in which a combination of both the Gabor path and texture-segmentation boundary were present and coincident (PTB) (see Figure 1).

Stimuli in all conditions were comprised of fields of Gabor patches. The Gabors had a carrier spatial frequency of six cycles per degree (c/°) chosen so that more than a full cycle was visible in a small patch. Shapes in the GP condition were defined by closed paths of Gabor patches. The gratings of the patches were aligned tangentially to the path. These paths were embedded in a uniform texture background also comprised of Gabor patches but with orientation of 45° with respect to the positive x-axis. Stimuli in the TB condition were closed shapes defined by the boundary between two textures that differed in the orientation of the Gabor patches that comprised them (a maximum orientation difference of 90° between inside and outside patches). This differs from Machilsen and Wagemans' (2011) study, which used random orientations in the surround, making the orientation coherence a cue. In our case, the locations of the orientation changes are also critical for the task. Stimuli in the PTB condition also had a 90° difference between the orientations of texture inside and outside the shape, and in addition had a sampled path demarcating the shape boundary (as in condition GP). For the first two experiments, the orientations of +45° and −45° for the texture patches was chosen to ensure equal contrast for the two different orientations since this matched and thus minimized adjacent pixel nonlinearities as a critical factor (Pelli & Zhang, 1991). Equation 1 defines the radial frequency contour used to create the borders in the stimuli:

$$R(\theta) = R_0 \times \Big(1 + A\sin(\omega\theta + \varphi)\Big) \quad (1)$$

in which $R(\theta)$ is the radius of the path at an angle of θ relative to the positive x-axis; R_0 (the base radius) is in all cases 4° of visual angle; A is the amplitude of distortion of a circle expressed as a proportion of R_0; ω is the frequency of modulation (RF number); and φ the phase of the modulation.

Each stimulus contained 4,225 Gabor patches systematically arranged in an implicit 65 × 65 square grid. The distance between grid lines was 16′. The Gabor patches were jittered at random within 6′ (vertically and horizontally) of their original position to degrade obvious alignment cues and give the appearance of a random arrangement of patch positions (see Figure 1). The diameter of the envelope of each Gabor patch at half maximum contrast was 9.42′. The phase of the grating in each patch for the texture was randomly determined to be in either positive or negative sine phase, with the centre of each patch, therefore, at background luminance. In instances where patches overlapped, the luminance profiles were added. Overlapping was a consequence of having enough patches to obtain a sufficiently dense texture for texture-segmentation in the given space. No additional informative cues were introduced from the overlapping of patches.

The boundary of the shape in all conditions conformed to Equation 1 with a base radius of 4° of visual angle. In condition TB, when the centre of the patches fell inside the shape they were given an orientation of 45°, and if they were outside the shape they were given an orientation of −45°. In conditions with Gabor patches aligned tangentially with the boundary (an explicit contiguous path: GP and PTB), the path was always composed of 64 patches (except in Experiment 4 where the path was composed of 32 patches): the shape boundary was specified and the 64 patches that were to represent the boundary were positioned at equal intervals of θ. The 64 patches in the grid closest to these positions were removed and replaced by the patches representing the boundary specified by Equation 1. The orientation of the carrier in these Gabor patches is given by the angle α, between the tangent to the path and the perpendicular to the local radius. In Equation 2, this orientation α was given by:

$$\alpha(\theta) = -\arctan\left(\frac{\omega A\cos(\omega\theta + \varphi)}{R(\theta)/R_0}\right) \quad (2)$$

with the meaning of parameters the same as in Equation 1. The phase of the shapes (their rotation) in all of the conditions was randomized.

Stimuli in Experiments 3 and 4 contained texture that had a spiral rotation. In all cases the orientation of

the elements in the spiral were at a 45° to the local radius.

Experiment 1

Procedure

The first task involved three of the five participants. In a two-interval forced choice (2IFC) task, participants were asked to determine which pattern was most deformed from circularity. Presentation of test and reference stimuli was randomized. Patterns were presented sequentially and each pattern appeared on screen for 160 ms with an interstimulus interval of 500 ms. The test stimulus in this task was an RF pattern that had 1, 2, or 3 CoM with a radial frequency of three cycles per 2π radians (subsequently referred to as RF3 modulation) and the rest of the contour was circular (see Figure 1); the reference stimulus was in all cases circular. Smoothing between the RF sections and circular sections of the contour was done by fitting a first derivative of a Gaussian (D1) to the transitional part of the sinusoidal modulation (Loffler et al., 2003). The method of constant stimuli was used to control stimulus presentation with nine different levels of amplitude modulation (A in Equation 1). Stimuli were presented 60 times at each of the nine levels per CoM for each condition, collected across three runs, including 4,860 trials in total.

Results

For each condition, the proportion of correct responses for the nine test amplitudes was calculated (for each individual). A Quick (1974) function (as shown in Equation 3) was fitted to the psychometric data to determine thresholds for the detection of the increment in amplitude:

$$p(A) = 1 - 2^{-\left(1+(A/\Delta)^{Q}\right)} \quad (3)$$

in which $p(A)$ is the probability of a correct response for an amplitude A; Δ is the threshold in A for discrimination of the test-pattern from the circular reference-pattern at a performance level of 75% correct; and Q is a measure of the slope of the psychometric function (Quick, 1974; Wilson, 1980).

Thresholds were measured for $n = 1$, 2, and 3 CoM on the completed pattern, and Δ decreased with the number of CoM at a rate of decrement conforming to a power function, where γ is the index of the power function and K is a parameter that represents the fitted value of threshold for a single CoM:

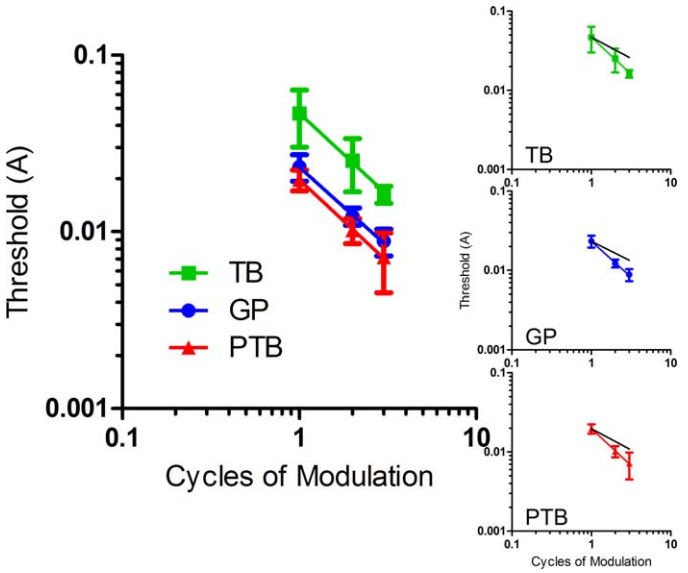

Figure 2. The figure on the left shows the mean thresholds for three participants versus the number of CoM plotted on logarithmic axes, so power function index equates to slope (with 95% confidence intervals). Figures on the right show each individual slope plotted with its respective prediction of probability summation (black line). TB = texture-segmentation boundary, GP = Gabor path, and PTB = Gabor path and texture-segmentation boundary. All slopes were observed to be steeper than their probability summation predictions.

$$\Delta(n) = K \times n^{-\gamma} \quad (4)$$

For each of the experimental conditions, Δ was plotted against CoM on logarithmic axes to render γ visible as the slope of a straight line (see Figure 2). The magnitude of the index of the power function γ predicted by probability summation is the reciprocal of the variable Q in the Quick function (Loffler et al., 2003; Quick, 1974; Wilson, 1980):

$$\gamma = \frac{1}{Q} \quad (5)$$

A rate of decrease greater than that predicted by probability summation [$\gamma > (1/Q)$] was indicative of global integration of signal across cycles.

Slopes of the fits all significantly exceeded their respective predictions of probability summation as can be seen in Figure 2: (TB) $\gamma = 0.93$ versus $1/Q = 0.53$; (GP) $\gamma = 0.90$ versus $1/Q = 0.50$; and (PTB) $\gamma = .93$ versus $1/Q = .54$. For comparisons of the observed slopes with their respective probability summation predictions using an extra sum of squares F-test (Motulsky, 2007), (TB) $F(1,7) = 15.32$, $p = 0.0058$; (GP) $F(1,7) = 68.06$, $p < 0.0001$; and (PTB) $F(1,7) = 55.27$, $p = 0.0001$.

Discussion

Past studies (Bell & Badcock, 2008; Hess & Field, 1999; Jeffrey et al., 2002; Loffler et al., 2003) have used the findings of steeper gradients for the fits to RF pattern threshold as a function of CoM than predicted by probability summation as an indicator of global pooling. In the current experiment, stimuli in all conditions were shown to have slopes that fell at a rate steeper than probability summation (as CoM increased). This indicates that the visual system was globally pooling the local cues around the shapes (for the current experiment) in order to detect deformation. The results also showed that observers were systematically better at discriminating shapes defined by a Gabor path over a shape defined by a difference in texture, even though the TB was composed of a maximum 90° orientation difference. Previous literature (Nothdurft, 1985, 1991) has shown that the strength of texture-segmentation is dependent on orientation contrast at the borders of the texture-shape to be detected, where increasing orientation differences increases the salience of the texture-segmentation. This is consistent with Field and colleagues' (1993) demonstration that collinear facilitation is minimal with large orientation changes between adjacent elements.

Experiment 2

Experiment 1 demonstrated that shapes defined by texture-segmentation and explicit paths of Gabor patches were both globally processed. The next thing we wanted to understand was how these global cues of texture-segmentation boundary and an explicit path interacted. It is possible that the two global shape cues are processed independently, in which case, the benefit to discrimination thresholds would only increase in a probabilistic manner (one cue from two cues); or, the two global shape cues could be processed by a single channel that would benefit from input from either cue. In this experiment, thresholds were determined for complete RF patterns (with three cycles of RF3 modulation) both in a conventional task (in which the observer was required to discriminate an RF pattern from a circle) and in an increment detection task (in which the observer was required to discriminate a pattern with a larger amplitude of modulation from a pattern with a predetermined pedestal level of modulation. It was anticipated that the relative strengths of the different cues would change with pedestal amplitude, leading to a strong test of the two predictions.

Procedure

In this experiment, an increment detection task was used which employed a 2IFC procedure. Stimuli in one interval had a base amount of amplitude modulation (A in Equation 1) that ranged from 0 to 0.06, while in the other interval an additional amount of amplitude modulation was added. In instances where the stimulus was not a circle, it was always an RF3 with 3 CoM. As before, participants were asked to determine which interval contained the pattern they perceived to be most deformed from circularity. The order of test and reference patterns was randomized. The display used identical durations of stimulus presentation and inter-stimulus intervals to the first experiment. The method of constant stimuli was employed, and there were 10,800 trials per observer (levels of additional amplitude modulation added to each pedestal amplitude [9] $\times$ stimuli presentations per level [20] $\times$ number of runs [4] $\times$ value of pedestal amplitude modulation [5] $\times$ stimuli condition [3]) The five different pedestal amplitudes were 0, 0.01, 0.02, 0.04, and 0.06 such that A in Equation 1 on any trial equals $A_b + \delta A$, where A_b is the baseline and δA is the increment in A from the baseline. The order of pedestal amplitude presentation was randomized across blocks. Runs were self-paced with breaks as necessary.

Results

Data was fitted with a Quick (1974) function specified by Equation 3 to obtain 75% threshold values. Figure 3 shows the mean threshold of the increment in amplitude plotted against pedestal amplitude for all five participants. Thresholds for TB (green square, $M =$ 0.016, 95% CI [0.012, 0.021]) were seen to be higher than those for GP (blue circle, $M = 0.011$, 95% CI [0.0064, 0.015]), which was also higher than those for PTB (red triangle, $M = 0.0095$, 95% CI [0.0057, 0.013]).

A 3 $\times$5 (stimulus-type $\times$ pedestal amplitude) repeated measures ANOVA showed that there were significant main effects of stimulus-type, $F(2, 12) =$ 13.1, $p = 0.001$, and pedestal amplitude, $F(4, 48) =$ 27.64, $p < 0.0001$. However, no interaction effect was observed, $F(8, 48) = 1.64$, $p = 0.14$. Planned-comparisons paired-samples t tests between the stimulus types showed that the thresholds of GP, PTB, and TB were all significantly different from each other, [GP vs. PTB, $t(4) = 4.34$, $p = 0.012$, $d = 0.43$; GP vs. TB, $t(4) = 4.59$, $p = 0.01$, $d = 1.42$; PTB vs. TB, $t(4) = 7$, $p = 0.002$, $d =$ 1.97; Cohen's d was used as a measure of effect size]. All tests were significant after a Bonferroni correction was applied.

Two predictions were generated for determining whether cues in the PTB stimuli were pooled into a

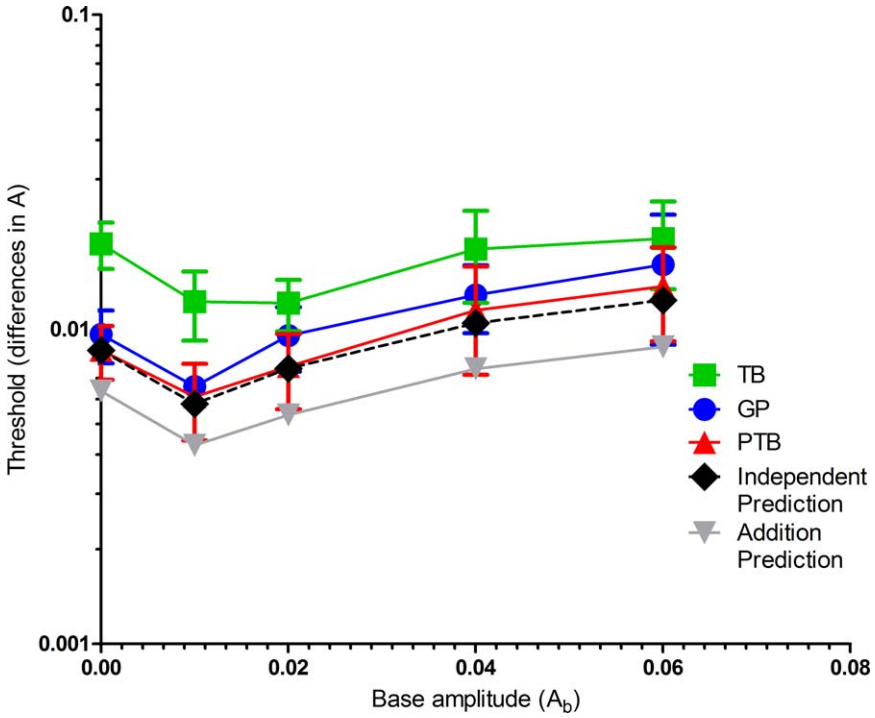

Figure 3. Mean thresholds on a logarithmic axis for five participants plotted against pedestal amplitude (with 95% confidence intervals). The legend shows the position of the lines from top to bottom on the graph. Prediction lines are described in the text.

common mechanism or whether they were independent. First, a prediction based on summing the cues of path and texture linearly was derived using (shown as the gray downward apex triangle in Figure 3):

$$\Delta A_{Add} = \frac{1}{\frac{1}{\Delta_{GP}} + \frac{1}{\Delta_{TB}}} \quad (6)$$

in which Δ is the threshold difference in A for discrimination of the test-pattern from the reference-pattern at a performance level of 75% correct and the subscript indicates the condition.

Second, a prediction for when the path and texture cues contribute independently to the threshold for the combined condition (shown as the black diamond in Figure 3) was derived using:

$$\Delta A_{Ind} = \frac{1}{\sqrt{\left(\frac{1}{\Delta_{GP}}\right)^2 + \left(\frac{1}{\Delta_{TB}}\right)^2}} \quad (7)$$

This is based on the notion that independent variables that combine separately to produce an overall detectability do so in a manner that conforms to an orthogonal vector sum (Massof & Starr, 1980). The PTB data was found to be significantly different from the addition prediction [$M = 0.0065$, $SD = 0.0018$, $t(4) = 5.11$, $p = 0.007$, $d = 1.22$] but not statistically different from the independent prediction [$M = 0.0089$, $SD = 0.0026$, $t(4) = 2.15$, $p = 0.098$, $d = 0.20$].

Discussion

In this experiment, an increment detection task was run to determine how adequately the predictions (assuming either independent cues or addition of cues) matched the outcome when the relative strengths of the two cues changed with pedestal amplitude. The data show that when both the TB and the GP are present on the same shape (i.e., PTB), thresholds for such a stimulus match predictions for a model that utilizes independent cues. Our findings seem to be in agreement with computational models in previous literature suggesting the autonomy of the mechanisms governing contour-defined and texture-defined shapes (Grigorescu, Petkov, & Westenberg, 2003) and also in human psychophysical adaptation studies (Gheorghiu & Kingdom, 2012a, 2012b; Kingdom & Prins, 2009). The data in Figure 3 also show that the plots have a "dipper" shape. This indicates that the small amount of signal present reduces the amount of additional signal required for discrimination of the test from the reference stimulus, hence resulting in a facilitation effect occurring at the "dip" (for an in-depth discussion of the "dipper" shape, see Bell, Wilkinson, Wilson, Loffler, & Badcock, 2009).

The lower thresholds obtained for PTB than for GP and TB was a significant effect in the current experiment and there was also a trend in the same direction in Experiment 1 (see Figures 2 and 3). Figure 2 shows that, within cues, all the shapes used were globally integrated

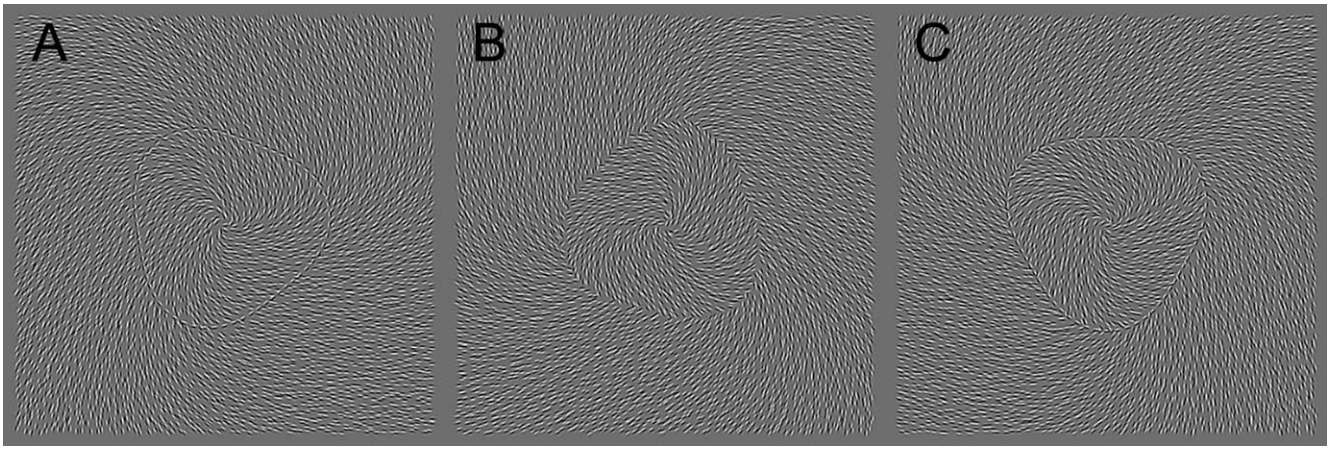

Figure 4. Examples of the conditions used with spiral texture: (A) GP shapes defined by a contiguous arrangement of Gabor patches, (B) TB shapes defined by texture-segmentation boundaries, and (C) PTB shapes defined by both an explicit Gabor path and texture-segmentation boundary. RF patterns shown here are at modulation amplitudes well above discrimination thresholds.

around the boundary of the shape when the base amplitude is zero. Figure 3 shows that the three data sets run in parallel from pedestal $A = 0$ to 0.06. It is tempting to assume that since global integration was obtained with $A = 0$ (see Figure 2), then it may also be present at nonzero amplitudes but additional tests do need to be conducted to confirm this.

It is, however, important to note that some sections of the path in the GP condition (even though the patches were still physically present) disappeared perceptually due to some of the patches on the path having orientations that were close to that of the background texture. Research has shown that when this occurs, a contour is not processed as a contour, but instead as part of the surrounding texture (Dakin & Baruch, 2009; Kingdom & Prins, 2009). Moreover, adaptation studies demonstrate that a reduced shape aftereffect is observed for a contour embedded in similar contours, despite the fact that the multicontour adaptor could potentially be a stronger adaptor than a lone contour (Gheorghiu & Kingdom, 2012b; Kingdom & Prins, 2009). However, template-based models of contour detection (Schmidtmann, Kennedy, Orbach, & Loffler, 2012) would still expect those patches to contribute to the global contour detection. This disappearance could have increased discrimination thresholds in the GP condition and could potentially alter predictions made. Experiment 3 uses modified stimuli to investigate whether our conclusions are compromised by this feature.

Experiment 3

In the previous experiment, the virtue of the diagonal texture was that the orientation variance was constant across the texture apart from at the boundary of the RF pattern, where there was a 90° orientation change. The drawback of this texture was that segments of the path of the GP stimulus were perceived to be disappearing into the background (as can be seen in Figure 1). In order to resolve this issue, we had to create another texture where there was the same orientation contrast at the RF pattern boundary, but made an angle to the path that was approximately constant to prevent the path from disappearing. To prevent this, a texture that did not fall into orientations similar to the path had to be created.

Examples of this new set of stimuli are depicted in Figure 4. Shapes were specified in an identical manner to that laid out in the General methods section above, with the only difference being that the texture had a spiral organization. This spiral texture was created so that the elements always had orientations approximately 45° to the path, hence maintaining the orientation contrast of the path to the texture on either side of the path. To be consistent with having a spiral background texture, TB had inner and outer textures of opposing spiral angles, one clockwise and one counterclockwise spiral. This was also used for the PTB condition. Although the orientation variance within small areas of the texture of this stimulus is different on either side of the texture boundary, apart from at the boundary itself, the variance changes smoothly and monotonically along a radius. The change in variance alone, therefore, cannot define a boundary.

Thresholds obtained from the spiral textured GP and TB stimuli would be used to make predictions for a linear addition or independent cue model (see Equations 6 and 7, respectively).

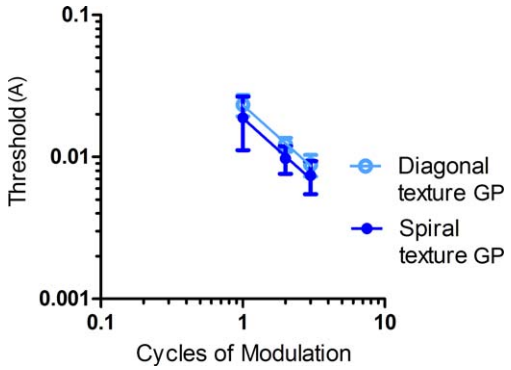

Figure 5. Comparison of thresholds for diagonal-textured GP and spiral-textured GP. Spiral-textured GP has lower overall thresholds than diagonal-textured GP but both have similar slopes.

Procedure

Procedure for this experiment was identical to that in Experiment 1.

Results

As with Experiment 1, a Quick (1974) function was fit to the psychometric data and the thresholds obtained were observed to conform to a power function when plotted against CoM.

The thresholds for the spiral-textured GP were lower than those for the diagonal-textured GP in Experiment 1 (see Figure 5). However, the gradients of the fits were not significantly different from each other, $F(1, 14) = 0.0099$, $p = 0.922$.

Slopes of the fits for all conditions in the current experiment were observed to be steeper than their respective probability summation prediction (see Figure 6): (TB) $\gamma = 0.93$ versus $1/Q = 0.57$; (GP) $\gamma = 0.89$ versus $1/Q = 0.52$; and (PTB) $\gamma = 0.97$ versus $1/Q = 0.54$. These slopes were all shown to be statistically different from the probability summation predictions, [(GP) $F(1, 7) = 11.28$, $p = 0.0121$; (TB) $F(1, 7) = 9.014$, $p = 0.0199$; and (PTB) $F(1, 7) = 14.42$, $p = 0.0067$].

Thresholds from the GP and TB conditions were used to calculate thresholds for the addition and independent predictions (as in Equations 6 and 7, respectively). On visual inspection, the fit for PTB seems to match the independent prediction (see Figure 7). However, the fit for PTB was not statistically significantly different from either the addition, $F(2, 8) = 3.96$, $p = 0.064$, or independent prediction, $F(2, 8) = 0.22$, $p = 0.81$.

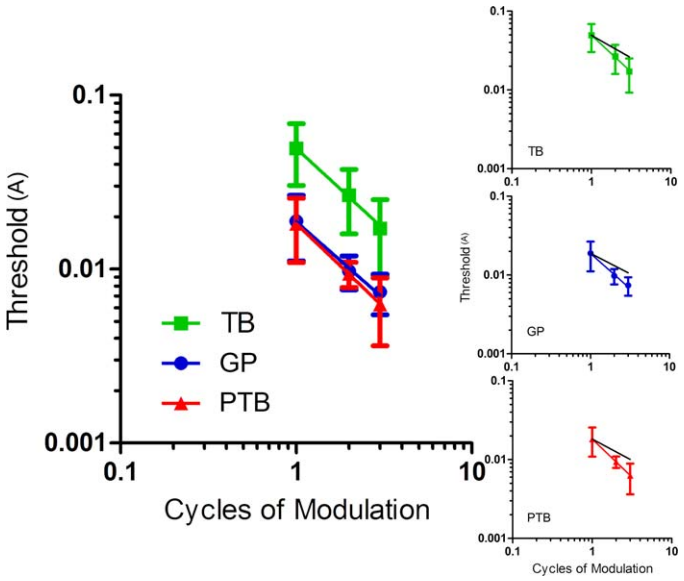

Figure 6. The figure on the left shows the mean thresholds (for three participants) versus the number of CoM plotted on logarithmic axes so power function index equates to slope (±95% confidence intervals). Figures on the right show each individual slope plotted with its respective prediction of probability summation (black line). GP = Gabor path, TB = texture-segmentation boundary, and PTB = Gabor path and texture-segment boundary. All slopes were observed to be steeper than their probability summation predictions.

Discussion

In this experiment, we succeeded in creating a GP stimulus that did not result in the disappearance of elements on the path and we noticed an improvement in discrimination ability in comparison to the previous diagonal-textured GP stimulus. Despite the change in the texture used, as before, all conditions were observed to have slopes steeper than their respective probability summation predictions, indicating global pooling around the shape. In Experiment 1, orientation variance of the diagonal texture was constant. For the

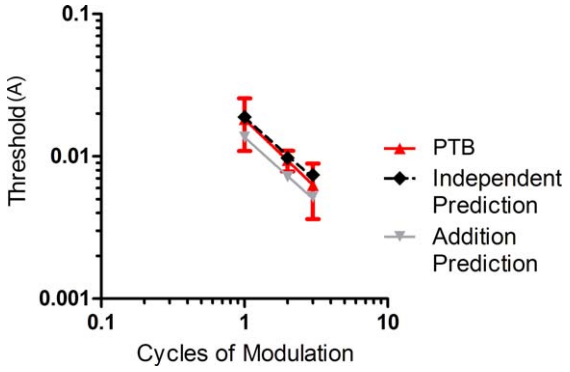

Figure 7. Mean thresholds for PTB compared with the independent and the addition prediction.

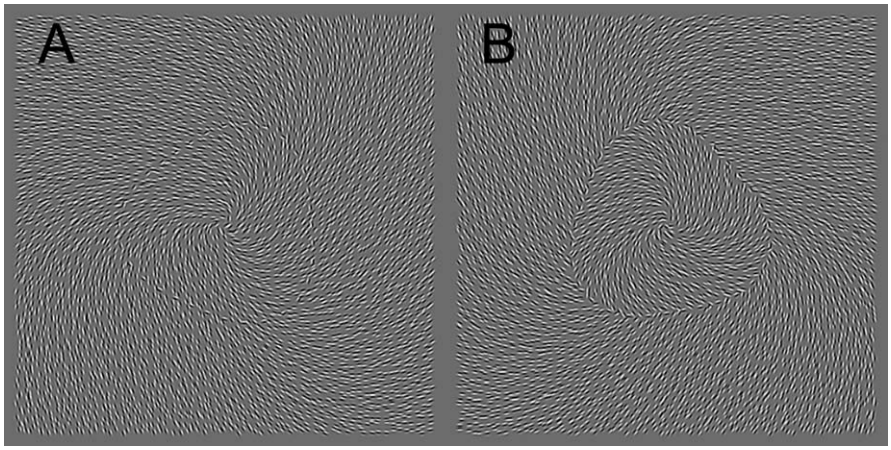

Figure 8. Example of the stimuli used in Experiment 4 that contain a Gabor path. The path contains half the number of elements as the equivalent conditions used in Experiment 3. (A) GP shapes defined by a contiguous arrangement of Gabor patches, and (B) PTB shapes defined by both an explicit Gabor path and texture-segmentation boundary.

current experiment however, there was a nonuniform orientation variance in the texture. Despite this difference in orientation variance, the same pattern of results (that the different stimuli used were globally processed) were observed, which demonstrates that the uniformity (or lack thereof) of orientation variance was not pertinent to global shape discrimination. In altering the texture to that of a spiral, we noticed that thresholds for the path in the GP stimulus were reduced relative to Experiment 1 (diagonal texture), and also that they became substantially lower than those of TB. The further apart the thresholds of the initial parameters (i.e., Δ_{GP} and Δ_{TB} in Equations 6 and 7) are, the closer the prediction thresholds for the independent and addition predictions become. This is likely to account for the failure to show any statistical differences between PTB and the addition prediction. The disparity in thresholds between GP and TB needs to be addressed to adequately test the prediction.

Experiment 4

In the previous experiment, using a spiral texture addressed the initial problem of the disappearance of elements on the path. However, it introduced another difficulty in that it increased the visibility of the GP stimulus such that thresholds for GP were more different from those of the TB stimulus than in Experiments 1 and 2, which, in turn, affected our ability to make useful predictions. In this experiment, we wanted TB and GP to be of comparable strengths to obtain better discrimination between the two predictions. McKendrick, Weymouth, and Battista (2010) have shown that reducing the number of patches defining a Gabor path embedded in a field of Gabors increases the observer's thresholds for discriminating the shape of a closed contour. In an attempt to increase discrimination thresholds of the Gabor path, the number of elements that made up the path (in GP and PTB conditions) was reduced prior to rerunning the procedure used in Experiment 3 (see Figure 8). Shapes in this experiment were created in the same way as in Experiment 3 except that paths in the GP and PTB conditions were created using half the number of Gabor patches (i.e., every second Gabor patch) present in the previous experiment, intervening patches had the orientation of the texture.

Procedure

Procedures for this experiment were the same as those in Experiment 3.

Results

A Quick (1974) function was fitted to the data and thresholds were observed to conform to a power function when plotted against CoM.

The alteration of the path in GP has equated the thresholds with those for TB (see Figure 9) and an extra sum of squares F-test showed that their fits were not statistically different from each other, $F(2, 14) = 0.78$, $p = 0.48$. Both fits of GP and TB were shown to be different from the fit of PTB, $F(2, 14) = 22.92$, $p < 0.0001$ and $F(2, 14) = 18.44$, $p = 0.0001$, respectively.

As shown in Figure 9, slopes for all conditions were seen to be steeper than their respective probability summation predictions: (TB) $\gamma = 0.93$ versus $1/Q = 0.57$, $F(1, 7) = 9.014$, $p = 0.0199$; (GP) $\gamma = 0.87$ versus $1/Q =$

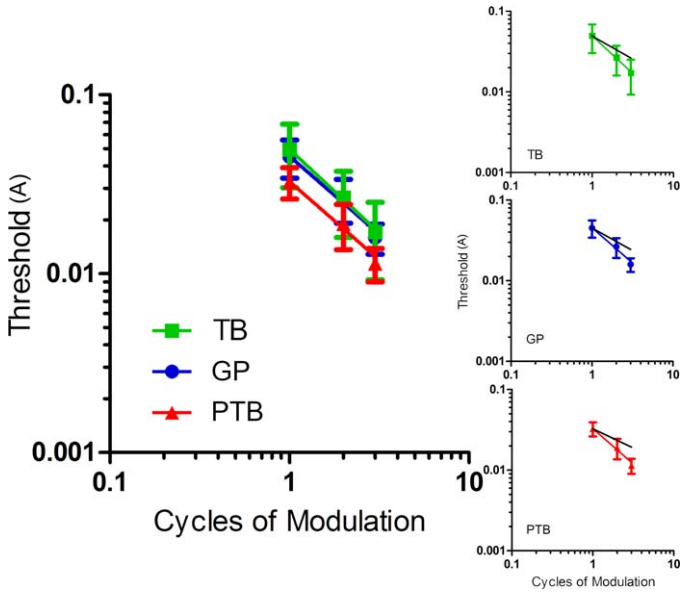

Figure 9. The figure on the left shows the mean thresholds for three participants versus the number of CoM plotted on logarithmic axes, so the power function is a straight line (with 95% confidence intervals). Figures on the right show each individual function plotted with its respective prediction of probability summation (black line). GP = Gabor path, TB = texture-segmentation boundary, and PTB = Gabor path and texture-segmentation boundary. GP and TB are observed to have thresholds that match, and all slopes are steeper than their probability summation predictions.

0.56, $F(1, 7) = 15.47$, $p = 0.0057$; and (PTB) $\gamma = 0.88$ versus $1/Q = 0.48$, $F(1, 7) = 29.74$, $p = 0.001$.

Thresholds from GP and TB were used to estimate thresholds for addition and independent predictions (see Figure 10). Visual inspection of the data shows that thresholds for PTB match those of the independent prediction, and this is supported by statistical tests showing no significant difference between PTB and the independent prediction ($F(2, 8) = 0.03521$, $p = 0.97$), and also that PTB is significantly different to the addition prediction ($F(2, 8) = 11.18$, $p = 0.0048$).

Discussion

In this experiment, we succeeded in reducing the thresholds of GP in comparison to TB by halving the number of patches that comprised the path. This resulted in the equal sensitivity to deformation in both the GP and TB. In comparing the PTB stimulus with the resultant predictions, we find that thresholds for a stimulus that comprises both a GP and a TB is best predicted by a model that suggests independent contributions from each global shape cue.

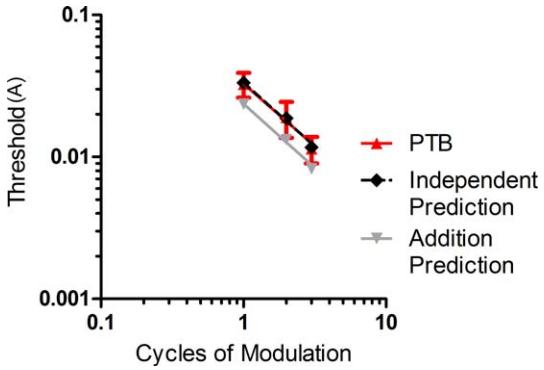

Figure 10. Mean thresholds for PTB compared with the independent and the addition prediction. PTB is significantly different from the addition prediction but the same as the independent prediction.

General discussion

To recapitulate, previous literature has shown that shape processing involves the initial detection of local contour orientation (Dickinson, Almeida, Bell, & Badcock, 2010; Loffler et al., 2003; Wang & Hess, 2005), estimation of local curvature (Bell et al., 2008; Bell et al., 2011; Poirier & Wilson, 2006); and global pooling of information in order to determine subtle changes in shape (Bell & Badcock, 2008; Dickinson, McGinty, Webster, & Badcock, 2012; Hess & Field, 1999; Jeffrey et al., 2002; Loffler et al., 2003). While this has been shown to occur for shapes defined by an explicit boundary of either contiguous elements or a connected contour (Dickinson, Han et al., 2010; Loffler et al., 2003), it had not been shown to occur for shapes defined by texture-segmentation boundaries. The results obtained in this study have been able to replicate previous studies (Bell & Badcock, 2008; Dickinson, McGinty et al., 2012; Jeffrey et al., 2002; Loffler et al., 2003) showing that detecting deformation of a shape improves at a rate that exceeds probability summation when CoM are systematically added to a circle for shapes defined by a continuous path of elements (GP). We were also able to demonstrate that this enhanced rate of improvement was apparent for shapes defined by texture-segmentation boundaries (TB). This suggests that like shapes defined by a first order cue, information around texture-segmentation-defined shapes are also pooled and processed globally. In comparing thresholds for the GP stimulus in Experiment 1 and Experiment 3, it is clear that, while thresholds for the GP stimulus that had perceptually disappearing patches on the path were indeed higher (i.e., the observer was not as sensitive to discriminating the shape when the patches were being perceived as background texture), it should be noted that the

gradients of their slopes were similar. This indicated that despite not having a perceptually "complete" shape (as is the case in Experiment 1), the visual system is still able to pool the local information and treat the shape as a whole. Global integration, as indicated by the slopes of the line, may still be occurring because the signal for the shape is present and the visual system might be detecting it in spite of the observer's inability to perceive the path at all locations. In moving from Experiment 1 to Experiment 3, the nature of the texture changed. The diagonal textures of Experiment 1 each have an orientation variance of zero in a Cartesian reference frame, and have maximally different orientations at the boundary. The orientation difference at the boundary between the two spiral textures of Experiment 3 is still maximal (the textures are still perpendicular at the boundary), but moving to a spiral texture introduces a radial gradient in orientation variance. The orientation variance within a fixed region is maximal at the center and reduces monotonically with radius (except, of course, when considering areas that encompass texture inside and outside of the texture boundary). If this additional cue differentiating the textures inside and outside of the boundary had affected thresholds it would have been in the direction of improving discrimination performance for both TB and PTB. However, as can be seen by comparing Figure 2 and Figure 6, the thresholds for TB were unchanged. The thresholds for the GP conditions were, however, improved, presumably because the whole of the path was now more visible. A consequence of this improvement in threshold was that the thresholds for the GP condition matched those of the spiral PTB condition, indicating that the Gabor path was so much more visible than the texture boundary that the texture boundary no longer contributed to performance in the discrimination tasks. It is not surprising then that under these circumstances that we again obtain global integration and thresholds for PTB that match an independent prediction. However, when we used spiral textures and matched the strengths of GP and TB (Experiment 4) we again achieved thresholds that conform to the prediction of independent mechanisms. These data suggest, therefore, that there is no evidence of strong fusion of an explicitly defined boundary and a texture-segmentation-defined boundary.

When both path-defined boundary and texture-segmentation-defined boundary are present and matched in their strengths, observers are better at discriminating a shape than with just the individual cues. Since the combined stimulus thresholds match the probability summation prediction (detecting one cue from two cues), we conclude that the lower thresholds for PTB are due to the availability of two cue types and not due to an additive combination of cues. While we do observe independent processing of texture-segmentation and explicitly defined boundaries, this does not conclusively indicate that two separate systems for shape are present in the human brain. The results are consistent with such a suggestion but the fact that we find that the boundaries are combined in a probabilistic manner would also suggest that the visual system, when presented with two choices of boundary types, picks one locally and uses the cue that it deems to be the stronger of the two. Although our data are consistent with the interpretation that an object might be defined by a texture-segmentation boundary or an explicit boundary, it could also be the case that the object boundary might be defined partly by texture-segmentation and partly explicitly. That is, that the different cues are assembled logically, using the strongest cue, into a boundary at a level in the processing hierarchy lower than that used to interpret shape. The global processing of shape might be agnostic to the nature of the boundary at the local level. Further studies are necessary to validate this.

It should be noted that previous studies using (sampled path) objects and differing textures have been conducted (Machilsen & Wagemans, 2011; Sassi, Machilsen, & Wagemans, 2012). However, these studies have looked at gross object shape detection and identification, rather than the discrimination of subtle changes to shape. Machilsen and Wagemans (2011) found that texture and explicit boundary cues were integrated for detecting the presence of shape. This differs from the current study, which involved a discrimination task. Additionally, it was unknown whether the shapes used in the previous study (Machilsen & Wagemans, 2011) were globally processed, whereas the current study employed the use of shapes for which global processing could be demonstrated. In their study, Sassi and colleagues (2012) used stimuli that either had one texture or two differing textures bounded by an explicit boundary and involved an identification and detection task. The stimuli that they used were outlines of everyday objects. In both studies, the cues were marked by orientation change relative to a random orientation surround and thus, orientation cues could drive a common mechanism. In our study, the path needed to be encoded precisely and, in one case, collinear facilitation would help (GP), whereas in the other, an orientation contrast was critical but collinear facilitation was likely to be minimal (TB). Furthermore, position information (of the boundary) was also required in the current study, and there is evidence to suggest that both position and orientation cues are used for global contour integration (Dickinson, Harman, Tan, Almeida, & Badcock, 2012; Wang & Hess, 2005).

This conclusion seems to be consistent with findings from neuroimaging studies in humans that have found that with some stimuli, object structure as defined by an

explicit boundary and objects defined by a texture boundary are processed in two different locations in the brain. While Kourtzi and Kanwisher (2000) observed activation in LOC for images of line drawings, Kastner, De Weerd, and Ungerleider (2000) observed V4 activation for the texture-defined boundaries. Indeed, a few psychophysical studies (Badcock et al., 2013; Dakin & Baruch, 2009; Gheorghiu & Kingdom, 2012b; Kingdom & Prins, 2009) have proposed that perhaps separate neural mechanisms exist for the processing of contour and texture.

In summary, the current study has demonstrated that like shapes defined by continuous paths of elements, shapes defined by differences in texture are also globally processed by a global shape detection mechanism. When both these cues are present on the same shape, the shape is still processed globally. However, while integration around the shape occurs regardless of how the shape is defined, we did not find integration across texture-segmentation boundary cues and an explicitly defined path when observers were discriminating shape. While we demonstrate that the mechanisms processing texture-segmentation boundaries and explicitly defined boundaries are separate and independent, it is as yet uncertain whether two independent processes for shape run from local to global. It might well be the case that the visual system uses a logical criterion for the selection of boundaries, which is then used for global processing.

Keywords: Shape, RF patterns, global pooling, texture segmentation, form

Acknowledgments

This research was supported by an Australian Research Council Grant DP1097003 to DRB, and a SIRF scholarship funded by the University of Western Australia to KWST.

Commercial relationships: none.
Corresponding author: Ken W. S. Tan.
Email: tanw06@student.uwa.edu.au.
Address: School of Psychology, The University of Western Australia, Crawley, Western Australia, Australia.

References

Badcock, D. R., Almeida, R. A., & Dickinson, J. E. (2013). Detecting global form: Separate processes required for Glass and radial frequency patterns. *Frontiers in Computational Neuroscience, 7*(53), 1–12.

Barbot, A., Landy, M. S., & Carrasco, M. (2012). Differential effects of exogenous and endogenous attention on second-order texture contrast sensitivity. *Journal of Vision, 12*(8):6, 1–15, http://www.journalofvision.org/content/12/8/6, doi:10.1167/12.8.6. [PubMed] [Article]

Bell, J., & Badcock, D. R. (2008). Luminance and contrast cues are integrated in global shape detection with contours. *Vision Research, 48,* 2336–2344.

Bell, J., Dickinson, J. E., & Badcock, D. R. (2008). Radial frequency adaptation suggests polar-based coding of local shape cues. *Vision Research, 48,* 2293–2301.

Bell, J., Gheorghiu, E., Hess, R. F., & Kingdom, F. A. A. (2011). Global shape processing involves a hierarchy of integration stages. *Vision Research, 51,* 1760–1766.

Bell, J., Wilkinson, F., Wilson, H. R., Loffler, G., & Badcock, D. R. (2009). Radial frequency adaptation reveals interacting contour shape channels. *Vision Research, 49*(18), 2306–2317.

Bergen, J. R. (1991). Theories of visual texture perception. In D. Regan (Ed.), *Vision and visual dysfunction: Spatial vision* (Vol. 10, pp. 114–134). London: The Macmillan Press Ltd.

Biederman, I. (1987). Recognition-by-components: A theory of human image understanding. *Psychological Review, 94*(2), 115–147.

Caputo, G. (1996). The role of the background: Texture segregation and figure–ground segmentation. *Vision Research, 36*(18), 2815–2826.

Dakin, S. C., & Baruch, N. J. (2009). Context influences contour integration. *Journal of Vision, 9*(2):13, 1–13, http://www.journalofvision.org/content/9/2/13, doi:10.1167/9.2.13. [PubMed] [Article]

Dickinson, J. E., Almeida, R. A., Bell, J., & Badcock, D. R. (2010). Global shape aftereffects have a local substrate: A tilt aftereffect field. *Journal of Vision, 10*(13):5, 1–12, http://www.journalofvision.org/content/10/13/5, doi:10.1167/10.13.5. [PubMed] [Article]

Dickinson, J. E., Bell, J., & Badcock, D. R. (2013). Near their thresholds for detection, shapes are discriminated by the angular separation of their corners. *PLoS One, 8*(5), 1–9.

Dickinson, J. E., Han, L., Bell, J., & Badcock, D. R. (2010). Local motion effects on form in radial frequency patterns. *Journal of Vision, 10*(3):20, 1–

15, http://www.journalofvision.org/content/10/3/20, doi:10.1167/10.3.20. [PubMed] [Article]

Dickinson, J. E., Harman, C., Tan, O., Almeida, R. A., & Badcock, D. R. (2012). Local contextual interactions can result in global shape misperception. *Journal of Vision, 12*(11):3, 1–20, http://www.journalofvision.org/content/12/11/3, doi:10.1167/12.11.3. [PubMed] [Article]

Dickinson, J. E., McGinty, J., Webster, K. E., & Badcock, D. R. (2012). Further evidence that local cues to shape in RF patterns are integrated globally. *Journal of Vision, 12*(12):16, 1–17, http://www.journalofvision.org/content/12/12/16, doi:10.1167/12.12.16. [PubMed] [Article]

Field, D. J., Hayes, A., & Hess, R. F. (1993). Contour integration by the human visual system: Evidence for a local "association field." *Vision Research, 33*(2), 173–193.

Gheorghiu, E., & Kingdom, F. A. A. (2012a). Chromatic properties of texture-shape and of texture-surround suppression of contour shape mechanisms. *Journal of Vision, 12*(6):16, 1–17, http://www.journalofvision.org/content/12/6/16, doi:10.1167/12.6.16. [PubMed] [Article]

Gheorghiu, E., & Kingdom, F. A. A. (2012b). Local and global components of texture-surround suppression of contour-shape coding. *Journal of Vision, 12*(6):20, 1–19, http://www.journalofvision.org/content/12/6/20, doi:10.1167/12.6.20. [PubMed] [Article]

Grigorescu, C., Petkov, N., & Westenberg, M. A. (2003). Contour detection based on nonclassical receptive field inhibition. *IEEE Transactions on Image Processing, 12*(7), 729–739.

Harrison, S. J., & Keeble, D. R. T. (2008). Within-texture collinearity improves human texture segmentation. *Vision Research, 48*(19), 1955–1964.

Heinrich, S. P., Andrés, M., & Bach, M. (2007). Attention and visual texture segregation. *Journal of Vision, 7*(6):6, 1–10, http://www.journalofvision.org/content/7/6/6, doi:10.1167/7.6.6. [PubMed] [Article]

Hess, R. F., & Field, D. J. (1999). Integration of contours: New insights. *Trends in Cognitive Sciences, 3*(12), 480–486.

Hussain, Z., Sekuler, A. B., & Bennett, P. J. (2011). Superior identification of familiar visual patterns a year after learning. *Psychological Science, 22*(6), 724–730.

Jeffrey, B. G., Wang, Y.-Z., & Birch, E. E. (2002). Circular contour frequency in shape discrimination. *Vision Research, 42*(25), 2773–2779.

Julesz, B. (1981). Textons, the elements of texture perception, and their interactions. *Nature, 290,* 91–97.

Kastner, S., De Weerd, P., & Ungerleider, L. G. (2000). Texture segregation in the human visual cortex: A functional MRI study. *Journal of Neurophysiology, 83*(4), 2453–2457.

Kingdom, F. A. A., & Prins, N. (2009). Texture-surround suppression of contour-shape coding in human vision. *Neuroreport, 20*(1), 5–8.

Kourtzi, Z., & Kanwisher, N. (2000). Cortical regions involved in perceiving object shape. *The Journal of Neuroscience, 20*(9), 3310–3318.

Landy, M. S., Banks, M. S., and Knill, D. C. (2011). Ideal-observer models of cue integration. In J. Trommershäuser, K. P. Körding, & M. S. Landy (Eds.), *Sensory cue integration* (pp. 5–29). New York, NY: Oxford University Press Inc.

Landy, M. S., & Bergen, J. R. (1991). Texture segregation and orientation gradient. *Vision Research, 31*(4), 679–691.

Loffler, G. (2008). Perception of contours and shapes: Low and intermediate stage mechanisms. *Vision Research, 48,* 2106–2127.

Loffler, G., Wilson, H. R., & Wilkinson, F. (2003). Local and global contributions to shape discrimination. *Vision Research, 43*(5), 519–530.

Machilsen, B., & Wagemans, J. (2011). Integration of contour and surface information in shape detection. *Vision Research, 51*(1), 179–186.

Malik, J., & Perona, P. (1990). Preattentive texture discrimination with early vision mechanisms. *Journal of the Optical Society of America A, 7*(5), 923–932.

Marr, D., & Hildreth, E. (1980). Theory of edge detection. *Proceedings of the Royal Society of London. Series B. Biological Sciences, 207*(1167), 187–217.

Massof, R. W., & Starr, S. J. (1980). Vector magnitude operation in color vision models: Derivation from signal detection theory. *Journal of the Optical Society of America, 70*(7), 870–872.

McKendrick, A. M., Weymouth, A. E., & Battista, J. (2010). The effect of normal aging on closed contour shape discrimination. *Journal of Vision, 10*(2):1, 1–9, http://www.journalofvision.org/content/10/2/1, doi:10.1167/10.2.1. [PubMed] [Article]

Motulsky, H. J. (2007). *Prism 5 statistics guide*. San Diego, CA: GraphPad Software, Inc. Retrieved from www.graphpad.com

Nothdurft, H. C. (1985). Sensitivity for structure

gradient in texture discrimination tasks. *Vision Research, 25*(12), 1957–1968.

Nothdurft, H. C. (1991). Texture segmentation and pop-out from orientation contrast. *Vision Research, 31*(6), 1073–1078.

Nothdurft, H. C. (1993). The role of features in preattentive vision: Comparison or orientation, motion and color cues. *Vision Research, 33,* 1937–1958.

Nothdurft, H. C., Gallant, J. L., & Van Essen, D. C. (2000). Response profiles to texture border patterns in area V1. *Visual Neuroscience, 17,* 421–436.

Pelli, D. G., & Zhang, L. (1991). Accurate control of contrast on microcomputer displays. *Vision Research, 31*(7–8), 1337–1350.

Poirier, F. J. A. M., & Wilson, H. R. (2006). A biologically plausible model of human radial frequency perception. *Vision Research, 46*(15), 2443–2455.

Poirier, F. J. A. M., & Wilson, H. R. (2010). A biologically plausible model of human shape symmetry perception. *Journal of Vision, 10*(1):9, 1–16, http://www.journalofvision.org/content/10/1/9, doi:10.1167/10.1.9. [PubMed] [Article].

Quick, R. F. (1974). A vector-magnitude model of contrast detection. *Biological Cybernetics, 16*(2), 65–67.

Ramachandran, V. S., Gregory, R. L., & Aiken, W. (1993). Perceptual fading of visual texture borders. *Vision Research, 33*(5–6), 717–721.

Regan, D. (2000). *Human perception of objects: Early visual processing of spatial form defined by luminance, color, texture, motion, and binocular disparity*. Sunderland, MA: Sinauer Associates Inc.

Regan, D., & Hamstra, S. J. (1992). Dissociation of orientation discrimination from form detection for motion-defined bars and luminance-defined bars: Effects of dot lifetime and presentation duration. *Vision Research, 32*(9), 1655–1666.

Sassi, M., Machilsen, B., & Wagemans, J. (2012). Shape detection of Gaborized outline versions of everyday objects. *i-Perception, 3*(10), 745–764.

Schmidtmann, G., Kennedy, G. J., Orbach, H. S., & Loffler, G. (2012). Non-linear global pooling in the discrimination of circular and non-circular shapes. *Vision Research, 62,* 44–56.

Thielscher, A., & Neumann, H. (2003). Neural mechanisms of cortico-cortical interaction in texture boundary detection: A modeling approach. *Neuroscience, 122*(4), 921–939.

Wang, Y.-Z., & Hess, R. F. (2005). Contributions of local orientation and position features to shape integration. *Vision Research, 45*(11), 1375–1383.

Wilkinson, F., Wilson, H. R., & Habak, C. (1998). Detection and recognition of radial frequency patterns. *Vision Research, 38*(22), 3555–3568.

Wilson, H. R. (1980). A transducer function for threshold and suprathreshold human vision. *Biological Cybernetics, 38*(3), 171–178.

Zwickel, T., Wachtler, T., & Eckhorn, R. (2007). Coding the presence of visual objects in a recurrent neural network of visual cortex. *Biosystems, 89*(1–3), 216–226.